European Journal of Medicinal Chemistry 44 (2009) 4021–4027

Contents lists available at ScienceDirect

European Journal of Medicinal Chemistry

journal homepage: http://www.elsevier.com/locate/ejmech

Original article

Synthesis and characterization of rhenium and technetium-99m tricarbonyl complexes bearing the 4-[3-bromophenyl]quinazoline moiety as a biomarker for EGFR-TK imaging

Athanasia Bourkoula [a], Maria Paravatou-Petsotas [a,*], Apostolos Papadopoulos [a], Isabel Santos [c], Hans-Jurgen Pietzsch [d], Evangelia Livaniou [a], Maria Pelecanou [b], Minas Papadopoulos [a], Ioannis Pirmettis [a]

[a] Institute of Radioisotopes–Radiodiagnostic Products, National Centre for Scientific Research "Demokritos", 15310 Athens, Greece
[b] Institute of Biology, National Centre for Scientific Research "Demokritos", 15310 Athens, Greece
[c] Departamento de Química, ITN, Estrada Nacional 10, 2686-953 Sacavém Codex, Portugal
[d] Institute of Radiopharmacy, Forschungszentrum Dresden-Rossendorf, P.O. Box 510 119, 01314 Dresden, Germany

ARTICLE INFO

Article history:
Received 3 March 2009
Received in revised form
13 April 2009
Accepted 18 April 2009
Available online 3 May 2009

Keywords:
Technetium
Rhenium
4-Anilinoquinazoline
Tyrosine kinase inhibitors
Epidermal growth factor receptor

ABSTRACT

Aiming at the development of technetium-99m (^{99m}Tc) complexes for early detection and staging of EGFR positive tumors, the tyrosine kinase inhibitor 6-amino-4-[(3-bromophenyl)amino]quinazoline was derivatized with pyridine-2-carboxaldehyde to generate the imine 6-(pyridine-2-methylimine)-4-[(3-bromophenyl)amino]quinazoline suitable for reacting with the *fac*-$[^{99m}Tc(CO)_3]^+$ core as an *N,N* bidentate ligand. The labelling was performed in high yield (>90%) by ligand exchange reaction using *fac*-$[^{99m}Tc(OH_2)_3(CO)_3]^+$ as precursor. The ^{99m}Tc complex was characterized by comparative HPLC analysis using the analogous rhenium (Re) complex as reference. The Re complex was prepared by ligand exchange reaction using the *fac*-$[ReBr_3(CO)_3]^{2-}$ as precursor and was fully characterized by NMR and IR spectroscopies and elemental analysis. *In vitro* studies indicate that both the ligand and its Re complex inhibit the EGFR autophosphorylation (IC_{50}: 17 ± 3.7 and 114 ± 23 nM respectively) in intact A431 cells, bind the receptor in a reversible mode, and inhibit A431 cell growth (IC_{50}: 5.2 ± 1.1 and 2.0 ± 0.98 μM respectively). Biodistribution of the ^{99m}Tc complex in healthy animals showed a rather fast blood and soft tissue clearance between 1 and 15 min p.i. with excretion occurring mainly via the hepatobiliary system.

1. Introduction

The epidermal growth factor receptor (EGFR) belongs to the HER family of transmembrane receptors with intrinsic protein kinase activity involved in cell proliferation, differentiation, cell migration, metastasis, angiogenesis and reduced responses to chemotherapy. These receptors share a similar structure consisting of an extracellular ligand-binding domain, a short hydrophobic transmembrane region, and an intracellular cytoplasmic domain containing the locus for tyrosine kinase (TK) activity and regulatory functions. Interaction of EGFR with its natural ligands, such as the epidermal growth factor (EGF), leads to dimerization of the ligand–receptor complexes, followed by autophosphorylation of the receptor at the intracellular tyrosine kinase domain. The autophosphorylation serves as a biochemical trigger for several downstream signal transduction pathways. Since tyrosine phosphorylation is a primary pathway whereby mitogenic signals are transduced through the cell membrane to the nucleus, mutational activation or overexpression of receptor tyrosine kinases is linked to malignant transformations. In particular, overexpression of the EGFR and its enhanced signalling has been associated with the initiation, progression and invasiveness of a great spectrum of human cancers. Overexpression of EGFR occurs in almost 100% of the head and neck tumors, followed by pancreatic and renal cell carcinomas, colorectal, breast, ovarian, prostate, bladder, non-small-cell lung cancer, and glioblastomas, etc. Also high expression of EGFR is frequently observed in many different types of epithelial cancers [1,2].

Due to its properties, the EGFR emerged in recent years as an attractive target for the development of anticancer pharmaceuticals that can specifically bind the receptor and inhibit its TK activity and downstream signalling [1,3,4]. Monoclonal antibodies (MAbs) directed against the external domain of the receptor [5,6] and small-molecule TK inhibitors (TKIs) that bind to the intracellular

* Corresponding author. Tel.: +30 210 6503837; fax: +30 210 6524480.
E-mail address: mparavatou@rrp.demokritos.gr (M. Paravatou-Petsotas).

0223-5234/$ – see front matter © 2009 Elsevier Masson SAS. All rights reserved.
doi:10.1016/j.ejmech.2009.04.033

tyrosine kinase region [7–9] are two classes of drugs approved for clinical use or in preclinical/clinical development for this purpose. Small-molecule TKIs target the catalytic kinase domain of EGFR and bind to the ATP-binding pocket of the cytoplasmic part of the receptor to inhibit intracellular receptor autophosphorylation, thereby preventing the initiation of signalling cascade. Several classes of tyrosine inhibitors have been reported [10–12], among which the 4-anilinoquinazoline derivatives are the most potent and selective as well as the most investigated so far [13–18].

Furthermore, considerable interest arose in the use of radiolabelled EGFR inhibitors for molecular imaging of tumors overexpressing the EGFR receptor and even for tumor radiotherapy. Several reversible and irreversible inhibitors, particularly from the 4-anilinoquinazoline class, were labelled with positron emitters, such as fluorine-18, carbon-11 and iodine-124, and their potential as PET imaging agents was evaluated [19,20].

The almost ideal properties of ^{99m}Tc for SPECT imaging and its widespread availability in comparison to PET isotopes justify the search for ^{99m}Tc-labelled quinazolines. Recently, the synthesis and *in vitro* evaluation of Re and ^{99m}Tc complexes, in which the 4-anilinoquinazoline pharmacophore was coupled to tailor made chelators suitable for the stabilization of either the M^{III} (M = Re and ^{99m}Tc) core with a "4 + 1" mixed-ligand system or of the tricarbonyl *fac*-$[M^{I}(CO)_3]^+$core, were presented [21]. It was shown that the Re complexes retain to a substantial degree the pharmacological properties of the 4-anilinoquinazoline pharmacophore, despite the presence of their organometallic core. These encouraging results prompted us to continue the investigation for useful ^{99m}Tc probes for early detection and staging of EGFR positive tumors. In this study we present the synthesis, characterization and biological evaluation of new Re (**6**) and ^{99m}Tc (**7**) complexes with the 6-(pyridine-2-methylimine)-4-[(3-bromophenyl)amino]quinazoline (**5**) suitable for acting as a bidentate *N*,*N* chelator with the *fac*-$[M(CO)_3]^+$ (M = Re, ^{99m}Tc) core.

2. Results

2.1. Chemistry

2.1.1. Synthesis of 6-(pyridine-2-methylimine)-4-[(3-bromophenyl)amino]quinazoline (*5*)

Ligand **5** was synthesized by reacting 6-amino-4-[(3-bromophenyl)amino]-quinazoline (**4**) with pyridine-2-carboxaldehyde. The yield of the reaction was 70% and all analytical data were consistent with the expected structure. Compound **4** was synthesized in four steps starting from 4-hydroxyquinazoline, as depicted in Scheme 1. All compounds were characterized by ^{1}H NMR and elemental analysis.

2.1.2. Synthesis of the rhenium complex [ReBr(*5*)$(CO)_3$] (*6*)

The synthesis of complex **6** (Scheme 2) was effected by ligand exchange reaction using equimolar quantities of ligand **5** and the organometallic Re–tricarbonyl precursor $[NEt_4]_2[ReBr_3(CO)_3]$. HPLC analysis of the reaction mixture showed the formation of a single product with an R_t of 15.6 min, clearly differentiated from the R_t of the ligand at 14.2 min. Complex **6** was isolated as an orange powder in high yield (75%) and was fully characterized by IR and NMR spectroscopies and elemental analysis.

The same complex was also obtained by using a previously reported two step method [22,23]. In the first step pyridine-2-carboxaldehyde reacted with the precursor $[NEt_4]_2[ReBr_3(CO)_3]$ forming the intermediate complex **8** that was not isolated. In the second step 6-amino-4-[(3-bromophenyl)amino]quinazoline (**4**) was added to the reaction mixture. The reaction was monitored by HPLC where it was shown that after 17 h at room temperature complexation of **4** was almost quantitative. Complex **6** was isolated in high yield (75%) as orange crystals.

The infrared spectrum of complex **6** shows strong bands in the 2023–1903 cm^{-1} range, attributed to the symmetric and asymmetric stretch bands of the C≡O bond, demonstrating the presence of the tricarbonyl core in the molecule [21,24–27].

Complex **6** is stable in the solid state as well as in solution for months, as shown by HPLC and NMR.

2.2. NMR studies

^{1}H and ^{13}C chemical shift assignments for ligand **5** and complex **6** are reported in Table S1. The ^{1}H–^{13}C correlation (HSQC) spectrum of complex **6** is presented in Fig. 1. Coordination of the ligand around the metal core results in downfield shifts of 0.7 ppm for the imine H-6 proton and of 0.3–0.4 ppm for the protons of the pyridinyl moiety, in accordance with coordination of the imine and pyridinyl nitrogens. Smaller downfield shifts are also noted for the protons of the quinazolinyl moiety. In the ^{13}C spectrum of complex **6**, downfield shifts are noted for the carbons close to the coordinating nitrogens; e.g., the C-6 carbon of the imine moiety is shifted

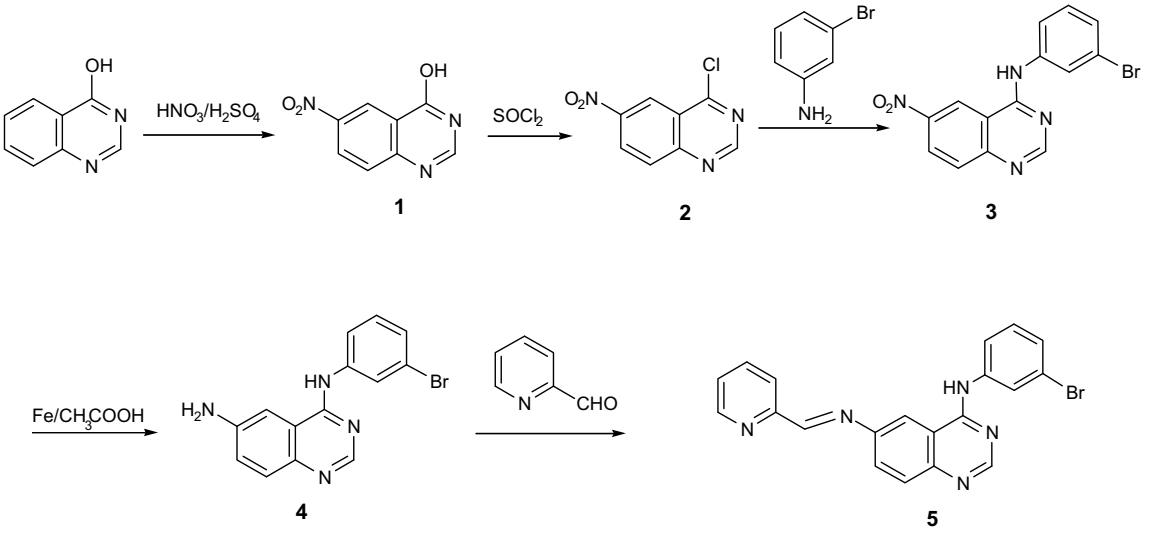

Scheme 1.

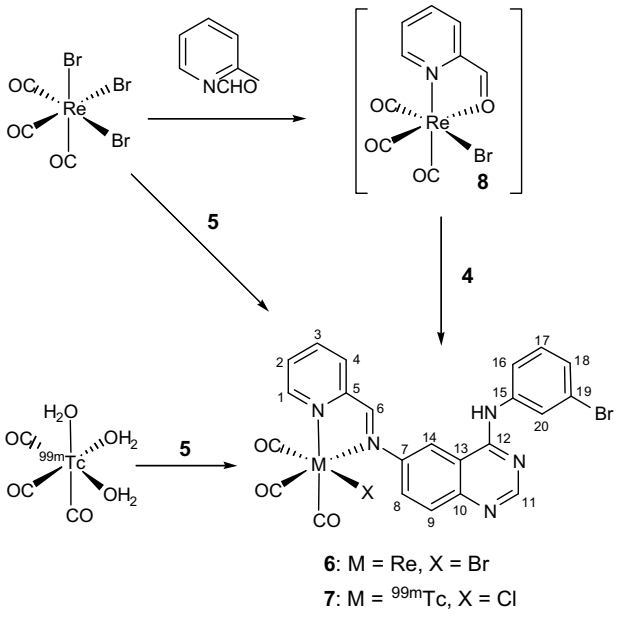

Scheme 2.

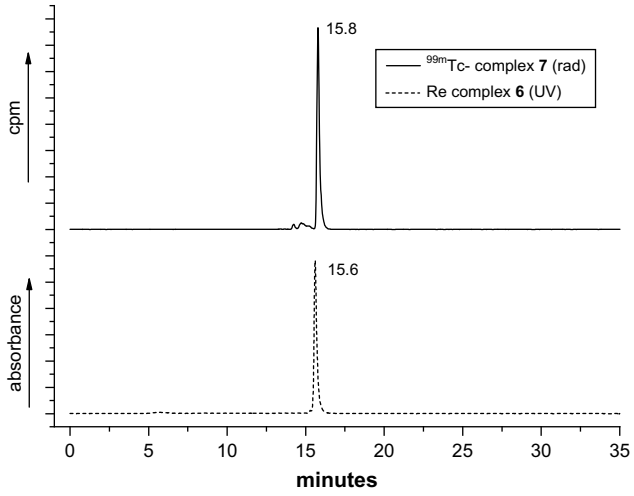

Fig. 2. Reverse phase HPLC chromatograms after injection of: (top) reaction mixture of labelling with ^{99m}Tc at RT for 20 min, gamma trace; (bottom) rhenium complex **6**, UV trace at 254 nm. Re complex **6** $R_t = 15.6$ min, ^{99m}Tc complex **7**: $R_t = 15.8$ min.

downfield by 8.4 ppm upon coordination. In addition, the three peaks at 186.7–196.9 ppm are characteristic for the presence of the tricarbonyl metal core and provide further evidence for the formation of the complex.

2.3. Preparation of ^{99m}Tc complex 7

Labelling of ligand **5** with ^{99m}Tc was carried out by ligand substitution using the *fac*-$[^{99m}Tc(OH_2)_3(CO)_3]^+$ tricarbonyl complex as precursor. The tricarbonyl precursor was prepared by the addition of pertechnetate to a commercially available Isolink kit that contains sodium boranocarbonate, which acts simultaneously as reductant and "in situ" source of CO [28]. The reaction was monitored by HPLC (R_t of pertechnetate 3.0 min, R_t of precursor 5.5 min, under the employed conditions) and was quantitative (>95%).

Reaction of ligand **5** with the precursor *fac*-$[^{99m}Tc(OH_2)_3(CO)_3]^+$ at room temperature for 20 min resulted in the formation of the ^{99m}Tc complex **7**. HPLC analysis showed the formation of a major product (85–90%) eluting at 15.8 min and a minor complex (~10%) eluting at 14.8 min (Fig. 2). Corroboration of the structure of the ^{99m}Tc complex was effected by comparative HPLC analysis using the analogous stable Re complex. As shown in Fig. 2 the Re complex elutes at 15.6 min; therefore the peak at 15.8 min is assigned to the analogous $[^{99m}TcCl(\mathbf{5})(CO)_3]$ complex **7** having a chlorine instead of bromine in the sixth coordination site.

The stability of the ^{99m}Tc complex **7** was monitored by HPLC for 24 h and no significant decomposition was observed (Table 1). Its stability in the presence of histidine and cysteine at a molar ratio of 1/1000 was also monitored by HPLC. As shown in Table 1, more than 90% of the complex remained intact after 24 h incubation with either cysteine or histidine.

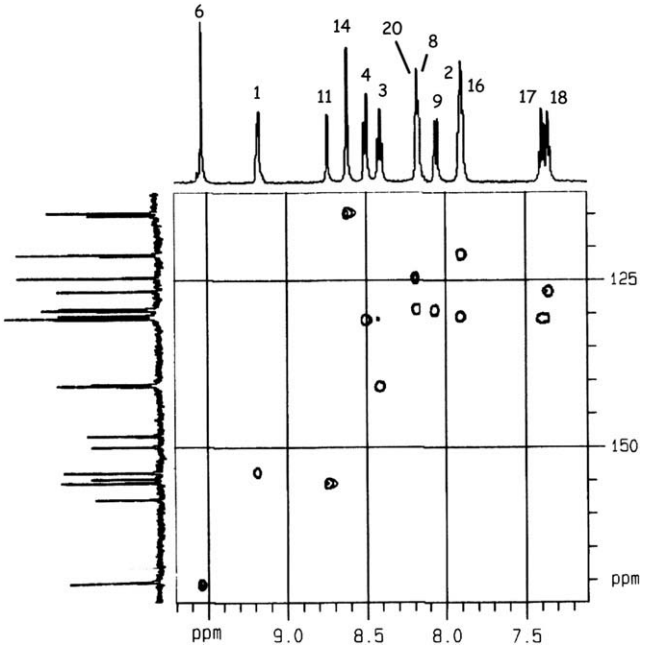

Fig. 1. ^{1}H–^{13}C correlation spectrum (HSQC, range δ_H 9.7–7.1, range 173.3–111.7) of complex **6** in DMSO-d_6 at 25 °C. The numbering of protons is shown in Scheme 2.

2.4. Biological evaluation

2.4.1. Inhibition of EGFR phosphorylation and reversibility tests

The compounds **4**–**6** were evaluated for their potency to inhibit EGFR phosphorylation in various concentrations by immunoblotting in intact A431 cells that overexpress the EGFR (Fig. 3). The percentage of EGFR phosphorylation was calculated and dose response curves were performed. IC_{50} values of the three compounds indicating the concentration (nM) needed to inhibit phosphorylation by 50% are presented in Table 2. In order to characterize the type of binding of the compounds as reversible or irreversible, the inhibition of phosphorylation was also determined

Table 1
Percentage of ^{99m}Tc complex **7** remaining intact after incubation with 1000 molar excess of histidine and cysteine at room temperature.

	Intact complex (%) after		
	1 h	4 h	24 h
None	99	98	96
Histidine	98	95	89
Cysteine	98	96	91

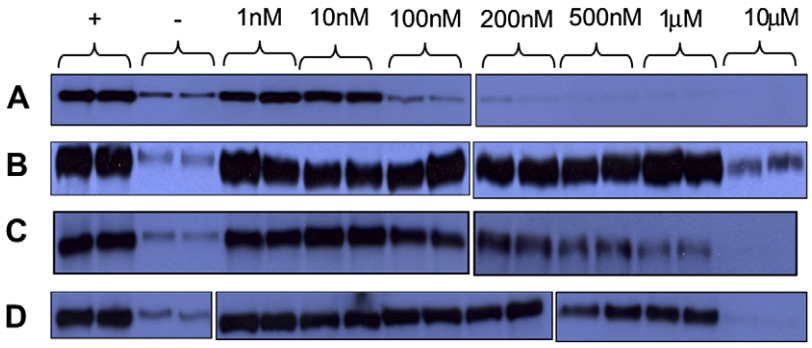

Fig. 3. Immunoblotting. The lines A and C represent the inhibition of the phosphorylation of EGFR immediately after removal of the compounds **5** and **6** respectively. The lines B and D represent the inhibition of the phosphorylation of EGFR 8 h after removal of the compounds **5** and **6** respectively.

8 h after the removal of the compounds and the IC_{50} values are also represented in Table 2.

2.4.2. In vitro inhibition of cell growth

The reference compound **4**, the ligand **5**, as well as its rhenium complex **6** were also evaluated for their potency to inhibit the A431 cell growth by the MTT assay. This assay measures the amount of MTT reduction by mitochondrial dehydrogenase and assumes that cell viability (corresponding to the reductive activity) is proportional to the production of purple formazan that is measured spectrophotometrically. Dose–response curves are presented in Fig. 4 and IC_{50} values in Table 2.

2.4.3. Biodistribution in mice

The *in vivo* distribution of the ^{99m}Tc complex **7** was evaluated in healthy mice at 1, 15, 60 and 180 min p.i. and data are summarized in Table 3. Complex **7** demonstrated a rather fast blood clearance between 1 and 15 min p.i. followed by a slower clearance between 15 and 180 min p.i. (21.51 ± 3.05%, 6.10 ± 0.63% and 2.01 ± 0.24% ID/g, at 1, 15 and 180 min p.i. respectively). Activity in the liver increases to 19.80 ± 1.55% ID/g, at 15 min and then decreases to 9.53 ± 1.65% ID/g, at 180 min p.i., while the activity in intestines increases up to 180 min p.i. The activity in the urine (and urinary bladder) and the stomach remained low during the study (4.60 ± 0.57%ID and 0.85 ± 0.37% ID/g, respectively, at 180 min p.i.).

3. Discussion

In the search for useful ^{99m}Tc probes for early detection and staging of EGFR positive tumors, we have designed and synthesized the new ligand **5** by combining a known tyrosine kinase inhibitor, the 6-amino-4-[(3-bromophenyl)amino]quinazoline (**4**), with pyridine carboxaldehyde via the formation of an imine. This ligand is expected to act as a bidentate chelator of the tricarbonyl *fac*-$[M(CO)_3]^+$ core with the N of pyridine and the N of imine acting as donor atoms. Tricarbonyl *N,N* complexes with other pharmacophore groups have been reported in the literature [23,29].

Spectroscopic and elemental analyses performed on the isolated Re complex showed that indeed ligand **5** acts as a bidentate chelator towards the *fac*-$[ReBr_3(CO)_3]^{2-}$ precursor and replaces two of the three bromine atoms, resulting in the formation of the desired neutral [ReBr(**5**)$(CO)_3$] complex **6**, as shown in Scheme 2. The chemistry was subsequently successfully transferred at tracer level to give the analogous [^{99m}TcCl(**5**)$(CO)_3$] complex **7** in high yield and radiochemical purity through the use of the $[^{99m}Tc(OH_2)_3(CO)_3]^+$ precursor. In the structure of **7** it is reasoned that the sixth position is occupied by a chlorine atom – present in the reaction medium – which replaces one of the H_2O ligands of the precursor. This replacement is a thermodynamically favoured process, resulting in an overall neutral complex [29,30]. The presence of chlorine is further supported by the high stability of complex **7** against histidine and cysteine challenge experiments (Table 1) given that the two ligands have very high affinity for the $[^{99m}Tc(CO)_3]^+$ core. The alternative presence of a water molecule at the sixth coordination site, which is easier to substitute due to electrostatic reasons, would have led in a high exchange with histidine or cysteine [31].

Biodistribution of the ^{99m}Tc complex in healthy animals (Table 3) showed a rather fast blood and soft tissue clearance between 1 and 15 min p.i. followed by a slower clearance between 15 and 180 min p.i. Excretion of the radioactivity occurred almost exclusively through the hepatobiliary system as evidenced by the decreasing activity in liver and the increasing amount of radioactivity in the intestine. At the same time the activity in the urine (and urinary bladder) was quite low. Stomach values at 180 min were low indicating minimal *in vivo* reoxidation to $^{99m}TcO_4^-$.

In the design of complexes **6** and **7** the chelating part does not interfere to a great extent with the biologically active quinazoline pharmacophore **4** [16] and is expected to present minimal steric hindrance to the interaction of the complexes with the intracellular domain of the EGFR. Indeed, the results obtained from the *in vitro* biological studies show that both ligand **5** and the rhenium complex **6** maintain the properties of the parent compound **4**. Specifically, they are able to cross the cell membrane of A431 cells significantly inhibiting the EGFR autophosphorylation and cell growth. Comparing ligand **5** to its rhenium complex **6** it is also apparent that the presence of the metal tricarbonyl core does not alter significantly the biological activity (IC_{50} 17 nM for **5** vs 114 nM for **6**). The activity of the rhenium complex, **6** is higher than the

Table 2
Inhibition of EGFR phosphorylation and inhibition of A431 cell growth by quinazoline derivatives **4**–**6**.

	Inhibition of phosphorylation		Inhibition of cell growth IC_{50}[c]
	Immediately after removal of the inhibitor IC_{50}[a]	8 h after removal of the inhibitor IC_{50}[b]	
4	3.5 ± 1.1 nM	>1 μM	4.8 ± 0.2 μM
5	17 ± 3.7 nM	>1 μM	5.2 ± 1.1 μM
6	114 ± 23 nM	>1 μM	2.0 ± 0.98 μM

IC_{50} values are represented as mean ± standard deviation.
[a] Concentration needed to inhibit by 50% the autophosphorylation of EGFR in A431 cells immediately after removal of the compound from the medium (detected by immunoblotting). Each experiment was performed twice in duplicate.
[b] Concentration (>1 μM) needed to inhibit by 50% the autophosphorylation of EGFR in A431 cells 8 h after removal of the compound from the medium (detected by immunoblotting). Each experiment was performed twice in duplicate. No exact IC_{50} values were estimated.
[c] Concentration needed to inhibit cell growth by 50%. Each experiment was performed twice in quadruple.

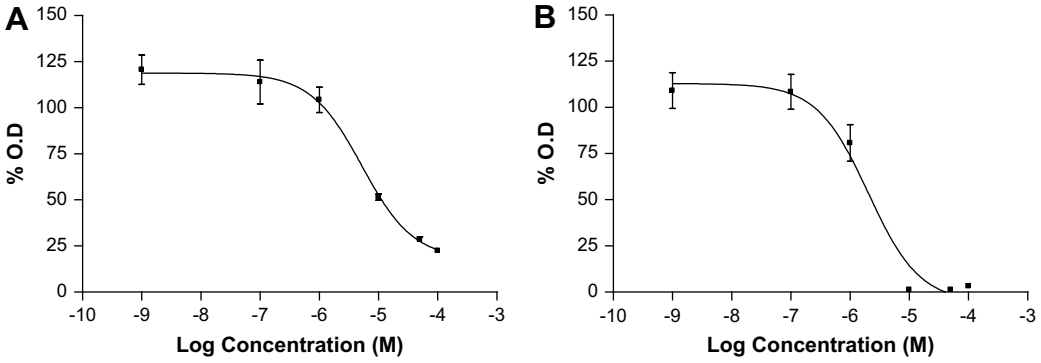

Fig. 4. MTT assay: dose–effect curves of (A): quinazoline derivative **5**, (B): quinazoline derivative **6**.

Table 3
Tissue distribution of radioactivity (%ID/g) after injection of [^{99m}TcCl(**5**)(CO)$_3$], **7** in mice.

Tissue	Time			
	1 min	15 min	60 min	180 min
Blood	21.51 ± 3.05	6.10 ± 0.63	4.33 ± 0.79	2.01 ± 0.24
Liver	8.24 ± 0.60	19.80 ± 1.55	13.77 ± 0.53	9.53 ± 1.65
Heart	3.86 ± 0.73	1.24 ± 0.21	1.21 ± 0.17	0.69 ± 0.12
Kidneys	7.29 ± 1.31	8.14 ± 0.62	7.49 ± 0.56	8.16 ± 0.90
Stomach	0.55 ± 0.03	0.85 ± 0.13	0.92 ± 0.11	0.85 ± 0.37
Intestine	0.79 ± 0.28	4.54 ± 0.57	11.90 ± 0.56	16.79 ± 1.19
Spleen	1.53 ± 0.34	2.05 ± 0.54	1.55 ± 0.22	0.82 ± 0.11
Muscle	0.83 ± 0.14	0.44 ± 0.06	0.41 ± 0.01	0.20 ± 0.04
Lungs	10.21 ± 3.22	3.14 ± 0.53	2.38 ± 0.51	1.62 ± 0.18
Brain	0.40 ± 0.06	0.13 ± 0.03	0.10 ± 0.02	–
Urine[a]	0.08 ± 0.03	1.57 ± 0.40	3.43 ± 0.56	4.60 ± 0.57

[a] Total excreted urine plus urinary bladder.

previously reported Re–tricarbonyl complexes (Table S2) [21] indicating an overall improvement in the design of the complexes.

According to the literature [10], quinazoline inhibitors of EGFR that have a Michael acceptor at the 6-position of quinazoline may bind irreversibly to the EGFR through formation of a covalent bond to Cys-773 located in the ATP-binding pocket. Since the presence of the imine bond at C-6 of the ligand **5** and complex **6** (Scheme 2) could in principle serve as a site of nucleophilic attack by the Cys 773 thiol, the mode of binding (reversible or not) of the **5** and **6** on EGFR was further investigated with *in vitro* experiments. It was found that phosphorylation of EGFR returns to control level 8 h after removing the inhibitors **5** and **6**, a fact that indicates their reversible binding (Fig. 3). This is in agreement with the lack of reactivity of the cysteine thiol against the ^{99m}Tc complex **7**, as witnessed in the cysteine challenge experiment. Apparently, complexes **6** and **7** act as reversible inhibitors since they bind non-covalently to the catalytic kinase domain of the EGFR.

The reference compound **4**, the ligand **5**, as well as its rhenium complex **6** were also evaluated for their potency to inhibit the A431 cell growth by the MTT assay (Fig. 4 and Table 2). The potency of ligand **5** (IC_{50}) is similar to that of the parent compound **4** (IC_{50} 5.2 μM and 4.8 μM respectively) while the Re complex **6** is slightly more potent with an IC_{50} value of 2.0 μM.

4. Conclusion

Overall, the biological evaluation of the novel complexes **6** and **7** with the bidentate ligand **5** as EGFR-TK inhibitors is promising and merits further exploration. This study, in combination with previous results on ^{99m}Tc-labelled quinazolines shows that attachment of the chelator part at the 6-amino position gives ligands and complexes that maintain the activity of the parent compound and this information may further be exploited in the design of new EGFR inhibitor ^{99m}Tc complexes.

5. Experimental protocols

5.1. Materials

All laboratory chemicals were reagent grade and were used without further purification. Solvents for high-performance liquid chromatography (HPLC) were HPLC-grade. They were filtered through membrane filters (0.22 μm, Millipore, Milford, MA) and degassed by a helium flux before and during use.

IR spectra were recorded as KBr pellets on a Perkin–Elmer 1600 FT-IR spectrophotometer in the region 4000–500 cm^{-1}. The NMR spectra were recorded on a Bruker 500 MHz Avance DRX spectrometer using $(CH_3)_4Si$ as the internal reference. Elemental analyses for C, H and N were conducted on a Perkin–Elmer 2400 automatic elemental analyzer. HPLC analysis was performed on a Waters 600 chromatography system coupled to both a Waters 2487 Dual λ Absorbance detector and a Gabi gamma detector from Raytest. Separations were achieved on a Nucleosil C18 (10 μm, 250 mm × 4 mm) column eluted with a binary gradient system at a 1 mL/min flow rate. Mobile phase A was methanol containing 0.1% trifluoroacetic acid, while mobile phase B was water containing 0.1% trifluoroacetic acid. The elution gradient was 0–1 min 100% B (0% A), followed by a linear gradient to 90% A (10% B) in 9 min; this composition was held for another 10 min. After a column wash with 95% A for 5 min, the column was re-equilibrated by applying the initial conditions (100% B) for 15 min prior to the next injection.

$Na^{99m}TcO_4$ was obtained in physiological saline as a commercial ^{99}Mo/^{99m}Tc generator eluate (Mallinckrodt Medical B.V., The Netherlands). The carbonyl labelling agent Isolink was provided by Mallinckrodt Medical B.V., The Netherlands. 6-Amino-4-[(3-bromophenyl)amino] quinazoline (**4**) and the rhenium precursor $[NEt_4]_2[ReBr_3(CO)_3]$ have been synthesized according to literature method [16,32,33]. The radioactive precursor *fac*-$[^{99m}Tc(OH_2)_3(CO)_3]^+$ was prepared using an Isolink kit (Mallinckrodt), according to the manufacturers.

5.2. Synthesis

5.2.1. Synthesis of 6-(pyridine-2-methylimine)-4-[(3-bromophenyl)amino]-quinazoline (*5*)

6-Amino-4-[(3-bromophenyl)amino] quinazoline (**4**) (1.0 g, 1.5 mmol) and pyridine-2-carboxaldehyde (1.5 mL) were transferred in a Dean–Stark apparatus containing 70 mL benzene. The mixture was boiled for 2 h and then the benzene was removed. The

yellow residue was washed with hot MeOH and dried under vacuum. Yield (834 mg, 65%); mp 233–234 °C. NMR assignment in Table S1. $C_{20}H_{14}BrN_5$ Anal. Calcd: C, 59.42; H, 3.49; N, 17.32. Found: C, 59.01; H, 3.44; N, 17.16. HPLC, t_R: 14.2 min.

*5.2.2. Synthesis of rhenium complex [ReBr(**5**)(CO)$_3$], (**6**)*

Method A. To a solution of $[NEt_4]_2[ReBr_3(CO)_3]$ (77 mg, 0.1 mmol) in 5 mL acetonitrile, **5** (40 mg, 0.1 mmol) was added under stirring. The solution was refluxed for 10 min, then 2 mL of distilled water was added and the mixture was refluxed for additional 30 min. After overnight standing at room temperature the precipitated dark orange solid was collected and recrystallized with hot acetonitrile. Yield: 52 mg, 69%. HPLC, t_R: 15.6 min.

Method B. To a solution of $[NEt_4]_2[ReBr_3(CO)_3]$ (154 mg, 0.2 mmol) in 5 mL methanol, pyridine-2-carboxaldehyde (21.4 mg, 19 μL) (0.2 mmol) was added under stirring. After 1 h a methanolic solution (5 mL) of 6-amino-4-[(3-bromophenyl)amino] quinazoline (62.3 mg, 0.2 mmol) was added and the solution was stirred at room temperature for 17 h. The orange precipitate formed was collected, washed with water and recrystallized from acetonitrile. Yield 114 mg, 76%. HPLC, t_R: 15.6 min.

Analysis for $C_{23}H_{14}Br_2N_5O_3Re$: C, 36.62; H, 1.87; N, 9.28; found: C, 36.30; H, 1.88; N, 8.98. IR (KBr, cm^{-1}): 2023 (s), 1920 (sh, s) and 1903 (br, s). NMR assignment in Table S1.

5.2.3. ^{99m}Tc-labelling

5.2.3.1. Preparation of fac-[^{99m}Tc(OH$_2$)$_3$(CO)$_3$]$^+$ *precursor.* ^{99m}Tc sodium pertechnetate (370–740 MBq, 1 mL) was added to the Isolink kit formulation (Mallinckrodt Medical B.V.) containing sodium tetraborate (2.9 mg), sodium carbonate (7.2 mg), sodium boranocarbonate decahydrate (2.85 mg) and sodium tartrate dihydrate (8.5 mg) and the mixture was incubated at 95 °C for 20 min. After cooling, 120 μL 0.1 N HCl was added and complex formation was checked by HPLC as described in Section 5.1. HPLC, t_R: 5.5 min.

*5.2.3.2. Synthesis of [^{99m}TcCl(**5**)(CO)$_3$], (**7**).* A solution (400 μL) of the *fac*-[^{99m}Tc(OH$_2$)$_3$(CO)$_3$]$^+$ precursor (pH 10) was added to a vial containing 400 μg of ligand **5**, dissolved in 400 μL acetonitrile. The solution was incubated at room temperature for 20 min. The reaction was monitored by HPLC that showed formation of one peak at 15.8 min. The identity of the complex was established by comparative HPLC studies using a sample of the well-characterized rhenium complex **6** as reference. The stability of the ^{99m}Tc complex at room temperature was studied by HPLC for a period up to 24 h.

5.2.3.3. Challenge with cysteine and histidine. Stability of complex **7** against trans-chelation was checked by cysteine and histidine challenge procedure. Aliquots of 100 μL of [^{99m}TcCl(**5**)(CO)$_3$] were added to 900 μL of a 10^{-2} M histidine and 10^{-2} M cysteine solution in saline, respectively. The samples were incubated at room temperature for 24 h. At various interval time points, 100 μL of each sample was removed and analyzed by HPLC, following the solvent system used for characterization of the complexes.

5.3. In vitro biological studies

5.3.1. Cell line

The human epidermoid vulval carcinoma A431 cell line [20], kindly provided by Dr E. Mishani (Hadassah Hebrew University, Israel), which overexpresses EGFR was used for the biological assays. Cells were maintained in high glucose D-MEM medium with L-glutamine (PAA Laboratories GmbH) and supplemented with 10% foetal bovine serum (PAA Laboratories GmbH) and penicillin/streptomycin (PAA Laboratories GmbH) 100 UI/100 μg per mL, in 5% CO_2 incubator at 37 °C.

5.3.1.1. Inhibition of EGFR phosphorylation in A431 cells and reversibility test protocols. A431 cells were seeded in duplicate in 6/well plates and grown to 70–80% confluence in supplemented D-MEM (high glucose). Next day, the cells were incubated in serum-free medium for 20 h. Afterwards, they were incubated for 2 h with varying concentrations of inhibitors (1 nM, 10 nM, 100 nM, 200 nM, 500 nM, 1 μM, 10 μM) and then treated as two different sets: the first set of cells was used to follow the inhibition of EGFR phosphorylation (inhibition test), while the second one was used to investigate whether the inhibition was reversible or irreversible (reversibility test).

To the first set of cells, EGF (20 ng/mL) was added for 5 min and then the cells were washed with PBS. Then, 0.2 mL of lysis buffer (50 mM Tris–HCl pH 7.4, 150 mM NaCl, 1% Triton X-100, 1 mM PMSF, 50 μg/mL aprotinin, 2 mM sodium orthovanadate, 50 μg/mL leupeptine and 5 mM EDTA) was added in each well and cell extracts were obtained by scraping cells with a rubber policeman and heating to 100 °C for 10 min. The second set of cells was washed with serum-free medium, incubated in D-MEM for 2 h, washed again with serum-free medium, incubated in D-MEM for another 2 h, washed with serum-free medium, incubated in D-MEM for another 4 h, and then stimulated with EGF (20 ng/mL) for 5 min. Afterwards, cell lysates were prepared as described for the first set of cells.

The total amount of protein in the cell lysates was determined by the BCA assay [34] in ELISA plates, using a BSA standard curve. Aliquots of each lysate corresponding to the same protein amount were loaded onto polyacrylamide gel (8%) and the proteins were separated by SDS-PAGE electrophoresis and subsequently transferred to a PVDF membrane. The membrane was immersed in Ponceau reagent (0.5% Ponceau in 1% acetic acid) for 5 min, washed with H_2O, blocked overnight with TTN containing 5% powdered milk (1% fat) and incubated 2 h with monoclonal anti-phosphotyrosine antibody diluted 1/2000 (PY20, Santa Cruz Biotechnology). The membrane was subsequently washed 3 times with TTN and incubated with a horseradish peroxidase-conjugated secondary anti-mouse IgG antibody diluted 1/3000 (Sigma) for 2 h and finally washed 3 times with TTN. Detection was performed using a chemiluminescent detection system according to the manufacturer's instructions (ECL kit, Amersham). Bands were quantified using the Band Leader version 3.00 program and the percentage of EGFR phosphorylation inhibition was calculated.

Both, inhibition and reversibility tests were performed twice for each of the three compounds **4**–**6**.

5.3.1.2. Cell proliferation assay. The A431 cells were seeded in 96-well plates at a density of 3000 cells per 100 μL per well and incubated for 24 h, so that they were attached to the wells. The day after seeding, exponentially growing cells were incubated with various concentrations of the quinazoline derivatives (ranging from 1 nM to 100 μM in quadruple) for 72 h. Control consisted of wells with no quinazoline derivatives added. The medium was removed and the cells were incubated for 4 h in the presence of 1 mg/mL MTT [35] (3-[4,5-dimethylthiazol-2-yl]-2,5-diphenyltetrazolium bromide, Sigma) in RPMI (PAA Laboratories GmbH) without phenol red for 2 h at 37 °C. The MTT solution was removed and isopropanol was added to each well to stop the cleavage of the tetrazolium ring by dehydrogenase enzymes which convert MTT to an insoluble purple formazan in living cells. Plates were then agitated at room temperature for about 15–20 min and the level of the coloured formazan derivative was determined by measuring optical density (OD) on an ELISA reader (540/620 nm). The results, which were expressed as: mean of the OD of various replicates × 100/OD of the control, were plotted against the corresponding compound concentration in a semi-log

chart and the IC_{50} was determined from the dose–response curve.

Cell proliferation assay was performed twice for each of the three compounds **4**–**6**.

5.4. Biodistribution studies in mice

Three groups of four Swiss Albino mice each (male, 30 ± 3 g) were injected with the ^{99m}Tc complex (0.1 mL, 1–2 μCi) through the tail vein. The animals of the first group were sacrificed by cardiectomy under slight ether anaesthesia 1 min after the injection, while the animals of the second and third group were sacrificed at 15 and 60 min post injection respectively. The organs of interest were excised, weighed and counted in an automatic gamma counter. Bladder and excreted urine were not weighed. The stomach and intestines were not emptied of food contents prior to radioactivity measurements. The percentage of injected dose per organ (%ID/organ) was calculated by comparison of sample radioactivity to standard solutions containing 10% of the injected dose. The calculation for blood and muscle was based upon measured activity, sample weight and body composition data (considering that blood and muscle comprise 7 and 43% of body weight). The percentage of injected dose per gram (%ID/g) was calculated by dividing the %ID/organ by the weight of the organ or tissue. All the animal experiments were carried out in compliance with the relevant national laws relating to the conduct of animal experimentation.

Acknowledgements

This project was part of an IAEA Coordinated Research Program "Development of ^{99m}Tc-based small bio-molecules using novel ^{99m}Tc cores". The authors thank Mallinckrodt Medical B.V., The Netherlands, for the Isolink boranocarbonate kits.

Appendix. Supplementary data

Detailed ^{1}H and ^{13}C assignments of compounds **5** and **6** in Table S1. Chemical structures and IC_{50} values of previously studied Re–quinazoline complexes [21] in Table S2. Supplementary data associated with this article can be found in the online version, at doi:10.1016/j.ejmech.2009.04.033.

References

[1] M. Sibilia, R. Kroismayr, B.M. Lichtenberger, A. Natarajan, M. Hecking, M. Holcmann, Differentiation 75 (2007) 770–787.
[2] P. Casalini, M.V. Iorio, E. Galmozzi, S. Menard, J. Cell. Physiol. 200 (2004) 343–350.
[3] R.D. Mass, Int. J. Radiat. Oncol. Biol. Phys. 58 (2004) 932–940.
[4] J.J. Laskin, A.B. Sandler, Cancer Treat. Rev. 30 (2004) 1–17.
[5] M. Peeters, J. Balfour, D. Arnold, Aliment. Pharmacol. Ther. 28 (2008) 269–281.
[6] J. Albanell, J. Codony, A. Rovira, B. Mellado, P. Gascon, Adv. Exp. Med. Biol. 532 (2003) 253–268.
[7] J. Smith, Clin. Ther. 27 (2005) 1513–1534.
[8] F. Hara, M. Aoe, H. Doihara, N. Taira, T. Shien, H. Takahashi, S. Yoshitomi, K. Tsukuda, S. Toyooka, T. Ohta, N. Shimizu, Cancer Lett. 226 (2005) 37–47.
[9] A. Sgambato, A. Camerini, B. Faraglia, R. Ardito, G. Bianchino, D. Spada, A. Boninsegna, V. Valentini, A. Cittadini, J. Cell. Physiol. 201 (2004) 97–105.
[10] A. Wissner, E. Overbeek, M.F. Reich, M.B. Floyd, B.D. Johnson, N. Mamuya, E.C. Rosfjord, C. Discafani, R. Davis, X. Shi, S.K. Rabindran, B.C. Gruber, F. Ye, W.A. Hallett, R. Nilakantan, R. Shen, Y.F. Wang, L.M. Greenberger, H.R. Tsou, J. Med. Chem. 46 (2003) 49–63.
[11] A. Wissner, P.R. Hamann, R. Nilakantan, L.M. Greenberger, F. Ye, T.A. Rapuano, F. Loganzo, Bioorg. Med. Chem. Lett. 14 (2004) 1411–1416.
[12] Y. Xia, C.D. Fan, B.X. Zhao, J. Zhao, D.S. Shin, J.Y. Miao, Eur. J. Med. Chem. 43 (2008) 2347–2353.
[13] A. Wissner, H.L. Fraser, C.L. Ingalls, R.G. Dushin, M.B. Floyd, K. Cheung, T. Nittoli, M.R. Ravi, X. Tan, F. Loganzo, Bioorg. Med. Chem. 15 (2007) 3635–3648.
[14] C.L. Arteaga, S.L. Moulder, F.M. Yakes, Semin. Oncol. 29 (2002) 4–10.
[15] V. Chandregowda, A.K. Kush, G. Chandrasekara Reddy, Eur. J. Med. Chem. 44 (2009) 3046–3055.
[16] G.W. Rewcastle, W.A. Denny, A.J. Bridges, H. Zhou, D.R. Cody, A. McMichael, D.W. Fry, J. Med. Chem. 38 (1995) 3482–3487.
[17] W.H. Ward, P.N. Cook, A. M Slater, D.H. Davies, G.A. Holdgate, L.R. Green, Biochem. Pharmacol. 48 (1994) 659–666.
[18] C.M. Discafani, M.L. Carroll, M.B. Floyd Jr., I.J. Hollander, Z. Husain, B.D. Johnson, D. Kitchen, M.K. May, M.S. Malo, A.A. Minnick Jr., R. Nilakantan, R. Shen, Y.F. Wang, A. Wissner, L.M. Greenberger, Biochem. Pharmacol. 57 (1999) 917–925.
[19] W. Cai, G. Niu, X. Chen, Eur. J. Nucl. Med. Mol. Imaging 35 (2008) 186–208.
[20] E. Mishani, G. Abourbeh, O. Jacobson, S. Dissoki, R. Ben Daniel, Y. Rozen, M. Shaul, A. Levitzki, J. Med. Chem. 48 (2005) 5337–5348.
[21] C. Fernandes, I.C. Santos, I. Santos, H.J. Pietzsch, J.U. Kunstler, W. Kraus, A. Rey, N. Margaritis, A. Bourkoula, A. Chiotellis, M. Paravatou-Petsotas, I. Pirmettis, Dalton Trans. (2008) 3215–3225.
[22] W. Wang, B. Spingler, R. Alberto, Inorg. Chim. Acta 355 (2003) 386–393.
[23] M.M. Saw, P. Kurz, N. Agorastos, T.S.A. Hor, F.X. Sundram, Y.K. Yan, R. Alberto, Inorg. Chim. Acta 359 (2006) 4087–4094.
[24] D.R. Gamelin, M.W. George, P. Glyn, F.W. Grevels, F.P.A. Johnson, W. Klotzbuecher, S.L. Morrison, G. Russell, K. Schaffner, J.J. Turner, Inorg. Chem. 33 (1994) 3246–3250.
[25] J. Granifo, Polyhedron 18 (1999) 1061–1066.
[26] P.A. Anderson, F.R. Keene, E. Horn, E.R.T. Tiekink, Appl. Organomet. Chem. 4 (1990) 523–533.
[27] E.W. Abel, K.G. Orrell, A.G. Osborne, H.M. Pain, V. Sik, M.B. Hursthouse, K.M. Abdul Malik, J. Chem. Soc., Dalton Trans. (1994) 3441–3449.
[28] R. Alberto, K. Ortner, N. Wheatley, R. Schibli, A.P. Schubiger, J. Am. Chem. Soc. 123 (2001) 3135–3136.
[29] R. Alberto, R. Schibli, A.P. Schubiger, U. Abram, H.-J. Pietzsch, B. Johannsen, J. Am. Chem. Soc. 121 (1999) 6076–6077.
[30] S. Mundwiler, M. Kundig, K. Ortner, R. Alberto, Dalton Trans. (2004) 1320–1328.
[31] R. Schibli, R. La Bella, R. Alberto, E. Garcia-Garayoa, K. Ortner, U. Abram, P.A. Schubiger, Bioconjug. Chem. 11 (2000) 345–351.
[32] J.S. Morley, J.C.E. Simpson, J. Chem. Soc. (1948) 360–366.
[33] R. Alberto, A. Egli, U. Abram, K. Hegetschweiler, V. Gramlich, P.A. Schubiger, J. Chem. Soc., Dalton Trans. (1994) 2815–2820.
[34] P.K. Smith, R.I. Krohn, G.T. Hermanson, A.K. Mallia, F.H. Gartner, M.D. Provenzano, E.K. Fujimoto, N.M. Goeke, B.J. Olson, D.C. Klenk, Anal. Biochem. 150 (1985) 76–85.
[35] R. Supino, in: S. O'Hare, C.K. Atterwill (Eds.), Methods in Molecular Biology, vol. 43, Humana Press, Totowa, NJ, 1995, pp. 137–149.